

## Intrinsic Route to Melt Fracture in Polymer Extrusion: A Weakly Nonlinear Subcritical Instability of Viscoelastic Poiseuille Flow

Bernard Meulenbroek,<sup>1,\*</sup> Cornelis Storm,<sup>1,†</sup> Volfango Bertola,<sup>2</sup> Christian Wagner,<sup>2</sup>  
Daniel Bonn,<sup>2</sup> and Wim van Saarloos<sup>1,2</sup>

<sup>1</sup>*Instituut-Lorentz, Universiteit Leiden, Postbus 9506, 2300 RA Leiden, The Netherlands*

<sup>2</sup>*Laboratoire de Physique Statistique, Ecole Normale Supérieure, 24 rue Lhomond, 75231 Paris Cedex 05, France*

(Received 14 February 2002; published 13 January 2003)

As is well known, the extrusion rate of polymers from a cylindrical tube or slit (a “die”) is in practice limited by the appearance of “melt fracture” instabilities which give rise to unwanted distortions or even fracture of the extrudate. We present the results of a weakly nonlinear analysis which gives evidence for an intrinsic generic route to melt fracture via a weakly nonlinear subcritical instability of viscoelastic Poiseuille flow. This instability and the onset of associated melt fracture phenomena appear at a well-defined ratio of the elastic stresses to viscous stresses of the polymer solution.

DOI: 10.1103/PhysRevLett.90.024502

PACS numbers: 47.20.Ft, 47.50.+d, 83.60.Hc

If a polymeric fiber is produced by extruding it from a so-called die, a cylindrical tube or planar slit, the surface often exhibits undulations or irregularities at higher flow rates; see Fig. 1. For increasing flow rates the undulations become progressively stronger, so much so that they can eventually cause the extrudate to break, hence the name *melt fracture*. A detailed understanding of this phenomenon has remained elusive for over 30 years.

Depending on the geometry and type of polymer, various types of phenomena seem to occur [2–4]. The short wavelength deformations of the interface often referred to as “sharkskin” instability appear to originate at the outlet: the extrudate quasiperiodically sticks to the outlet, widens, snaps loose, and narrows. In the “spurt-flow” regime, the extrudate shows intermittent bands of smooth and irregular surfaces; there is good evidence that this has to do with a stick-slip phenomenon at the wall of the die. In spite of the multitude of possibilities, there is every reason to believe that when these instabilities are absent, as in the experiments of Fig. 1, polymer flow still exhibits some elusive generic bulk flow instability: According to the engineering literature [4], a qualitative change in the flow behavior appears to occur at a more or less constant ratio of the normal stress difference of the melt over the shear stress for almost any polymer. Isolating this intrinsic mechanism is the main purpose of this Letter. Our contribution also opens up new avenues for a more general understanding of the rich variety of complex fluid flow instabilities, such as polymer turbulence [5] or the fact that complex fluids such as granular media are prone to shear banding in standard shear configurations.

The first linear stability analysis of the flow in the die of a viscoelastic fluid described by the so-called Oldroyd-B constitutive equations [6], performed some 25 years ago [7], showed that the flow was stable. Since then it has been generally accepted that *Poiseuille flow of viscoelastic fluids is linearly stable*. The absence of a clear *linear instability* explains the focus on other mechanisms, such

as those mentioned above. In this Letter we present the result of an analytical nonlinear amplitude expansion which shows that *viscoelastic Poiseuille flow exhibits a weakly nonlinear (or “subcritical”) instability* due to normal stress effects; this instability appears to make melt fracture phenomena unavoidable for polymer fluids with normal stress effects, even if care is taken to suppress instabilities associated with the wall or shape of the die. Recent experiments on polymers whose rheology is well captured by the Oldroyd-B model [1] confirm our scenario as well as our quantitative predictions.

Although polymer fluids can exhibit all kinds of complicated relaxation phenomena, the basic feature that essentially all polymer fluids (and in fact most complex fluids) share is the occurrence of elastic stress effects: when the shear rate is sufficiently strong that the polymers become stretched by the flow gradients, the forces along the normals of a little cubical fluid element are

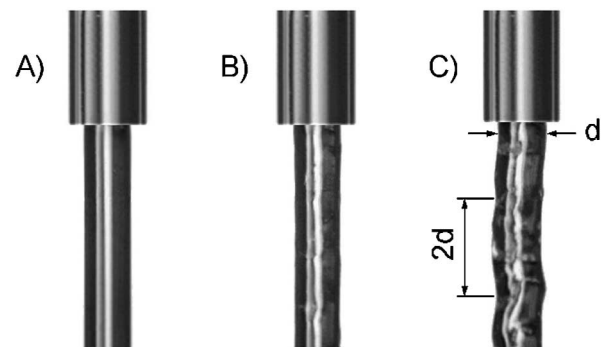


FIG. 1. Illustration of the surface irregularities that occur in the extrusion of a polymer fluid from a capillary tube (the wider structure at the top) in the absence of sharkskin or spurt-flow instabilities. For small speeds, the surface is smooth (a), but beyond some flow speed surface irregularities develop (b),(c). The wavelength is of the order of twice the diameter  $d$  of the capillary. After [1].

different in different directions, unlike what happens for a Newtonian fluid where the pressure is isotropic. Microscopically, this effect is due to the fact that in sufficiently strong shear flows the polymers get stretched (like little rubber bands) and acquire a nonisotropic orientational distribution. Thus they “pull” differently on fluid elements in the direction along the flow and along the shear gradient. The simplest model to capture this effect (and which hence has become the working horse of theoretical studies of viscoelastic polymer flow [6,8,9]) is the so-called Oldroyd-B model; we study it in the limit of large polymer viscosity, in which case it is referred to as the upper convected Maxwell (UCM) model. In this regime it is defined by the following constitutive equation for the shear stress tensor  $\boldsymbol{\tau}$  in terms of the velocity shear tensor  $\nabla\boldsymbol{v}$  through

$$\begin{aligned} \boldsymbol{\tau} + \lambda[\partial\boldsymbol{\tau}/\partial t + \boldsymbol{v} \cdot \nabla\boldsymbol{\tau} - (\nabla\boldsymbol{v})^\dagger \cdot \boldsymbol{\tau} - \boldsymbol{\tau} \cdot (\nabla\boldsymbol{v})] \\ = -\eta(\nabla\boldsymbol{v} + (\nabla\boldsymbol{v})^\dagger), \end{aligned} \quad (1)$$

This constitutive equation is characterized by one single relaxation time  $\lambda$ . The first two terms between square brackets together constitute the total time derivative of a fluid element moving with the flow; the other two nonlinear terms are required by frame independence, e.g., the fact that a solid-body rotation of the fluid does not lead to elastic stress effects. For fluids given by this constitutive equation, the velocity profile in Poiseuille flow is parabolic, just as in Newtonian fluids. Moreover, in a cylindrical tube with radius  $R$  and coordinates  $(\theta, r, z)$ , the above-mentioned Weissenberg number (also called the Deborah number), which is defined as

$$Wi \equiv \frac{\tau_{rr} - \tau_{zz}}{\tau_{rz}} \Big|_{\text{wall}}, \quad (2)$$

becomes, upon following the usual convention to denote the shear rate  $\partial v_z^{\text{unp}}/\partial r|_{\text{wall}}$  by  $\dot{\gamma}$ ,

$$Wi = 2\lambda\dot{\gamma} = 4v_{\text{max}}\lambda/R. \quad (3)$$

Note that the Weissenberg number defined in (2) is indeed the ratio of the so-called first normal stress difference  $\tau_{rr} - \tau_{zz}$  at the wall over the shear stress at the wall. Newtonian fluids are isotropic and hence the stress difference is zero; for Oldroyd-B model fluids the normal stress difference  $\tau_{rr} - \tau_{zz} \sim \dot{\gamma}^2$  [6], while the shear stress is linear,  $\tau_{rz} \sim \dot{\gamma}$ ; as a result  $Wi$  is simply linear in  $\dot{\gamma}$ .

The weakly nonlinear instability scenario that our calculations imply is illustrated in Fig. 2(a). Along the vertical axis we plot the relative perturbation of the basic flow profile (e.g., the relative shear perturbation at the wall, or the relative shear stress perturbation at the wall) as a function of  $Wi$ . Perturbations of the flow whose amplitude is bigger than the value given by the thick dashed line are unstable; their amplitude grows to some nonlinear value indicated by the full line. This line denotes nontrivial flow behavior with a characteristic wavelength. Note that the dashed line never touches the

horizontal axis, in agreement with the fact that Poiseuille flow is always linearly stable [7], although the threshold amplitude becomes very small for large  $Wi$ . Furthermore, note that the full line merges with the unstable (dashed line) branch (this is called a saddle-node bifurcation point in technical terms); below the corresponding value  $Wi_c$ , Poiseuille flow is nonlinearly stable to perturbations of any amplitude. In this Letter, we focus on our results for the cylindrical die, since this is the most relevant case. For slits similar results are obtained [10].

Figure 2(b) shows our analytical results for the (dashed line) branch that marks the threshold amplitude beyond which the flow is unstable. As described in more detail

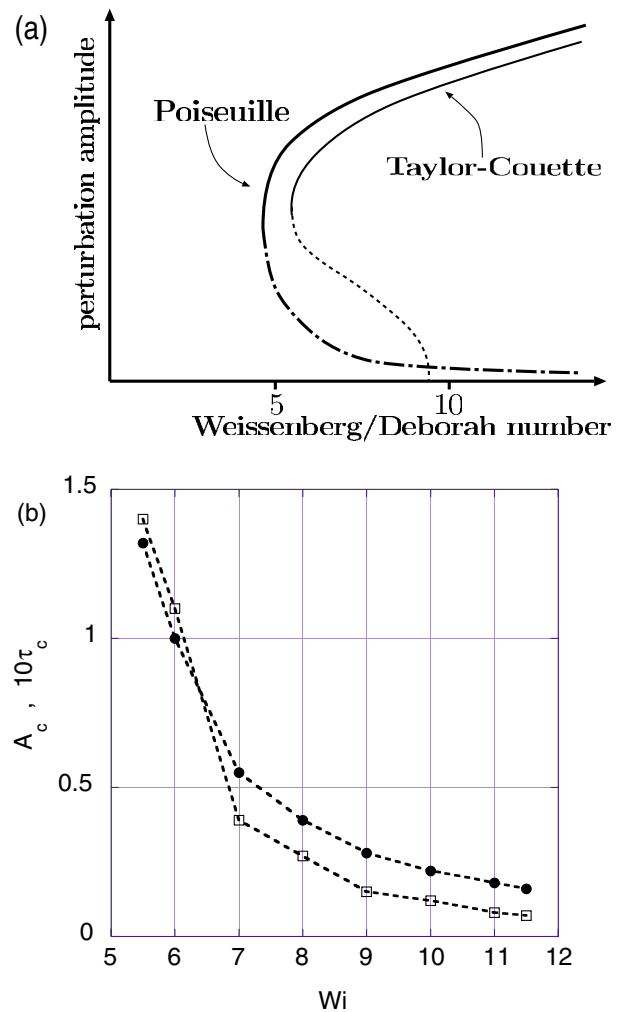


FIG. 2 (color online). Summary of our main result for the stability of viscoelastic Poiseuille flow in a cylinder in the zero Reynolds number limit. (a) Semiquantitative sketch of the bifurcation scenario. See text. (b) Our results for the threshold values of the amplitude beyond which the flow is unstable; these curves correspond to the dashed branch in (a). Dots indicate the critical value of the shear rate at the wall (normalized to the shear in the unperturbed case), and squares indicate the critical value of the relative shear stress perturbation, multiplied by 10.

below, our analysis is based on an expansion to third order in the perturbation amplitude; beyond some critical value  $Wi_c \approx 5$ , we find that the cubic terms in our expansion lead to an instability, and from this we are able to calculate the threshold value. Clearly, our results are fully consistent with the scenario of Fig. 2(a): the flow is stable to arbitrarily small (linear) perturbations, but perturbations as small as a few percent in the shear stress at the wall already render the flow unstable for values of  $Wi$  around 10. The critical value of  $Wi_c$  we estimate from our calculations is also in agreement with the very recent experimental data on a model UCM fluid [1], and with the range where long polymers have been reported to show a change in the flow behavior [4].

Actually, a number of observations already made us believe that the scenario summarized in Fig. 2 was a viable one before we embarked on our analysis: (i) For increasing  $Wi$ , the linear stability actually becomes arbitrarily weak (the damping of the linear modes decreases as  $1/Wi$ ). (ii) In the zero Reynolds number limit, the flow of an Oldroyd-B fluid in a Taylor-Couette cell (two concentric rotating cylinders) is linearly unstable above some well-defined value of the Deborah number, which is analogous to the Weissenberg number [8,9]. This linear instability is due to the fact that “hoop stresses” generally make flow along curved streamlines unstable [8,11]. However, recent experimental investigations [12] have clearly demonstrated that the instability is subcritical: as sketched qualitatively in Fig. 2(a), the nonlinear flow branch corresponding to roll-type patterns in the Taylor-Couette cell has been shown [12] to extend down to about half the critical value where the linear instability occurs (the point where the dotted line intersects the horizontal axis). The subcritical character of the instability has been argued not to depend on the curvature of the streamlines which causes the linear instability in the Taylor-Couette cell. Thus, it is reasonable to assume that both in viscoelastic Poiseuille flow and in viscoelastic Taylor-Couette flow there is a subcritical instability, and that the only essential difference is that in the first case the dashed branch never intersects the horizontal axis, while in the second case it does. (iii) The transition to turbulence for Poiseuille flow of Newtonian fluids is also subcritical [13].

Returning to our analysis, it is based on deriving the first nontrivial nonlinear term in an amplitude expansion for the perturbation to the velocity and shear stress fields of Poiseuille flow of an UCM fluid. We write the constitutive equation (1) and the Navier-Stokes equation in cylindrical coordinates and then study the evolution of the amplitude  $A$  of a perturbation  $A(\delta v_r, \delta v_z, \delta \tau_{\theta\theta}, \delta \tau_{rr}, \delta \tau_{rz}, \delta \tau_{zz})e^{ikz-i\omega t}$ , where the vector is normalized such that the shear perturbation  $\partial \delta v_z / \partial r$  at the wall equals  $A$ . To first nontrivial order we then obtain an equation of the form

$$dA/dt = -i\omega(k)A + c_3|A|^2A + \dots \quad (4)$$

To linear order in  $A$  this equation simply reproduces the

term  $\omega(k)$  of the dispersion relation of a single mode  $e^{ikz-i\omega t}$ ; this term is already contained in the old analysis of [7]. In particular, since we know that every mode  $k$  is linearly stable,  $\text{Im}\omega(k) < 0$  for all  $k$ .

The crucial new feature of our analysis consists of calculating the coefficient  $c_3$  explicitly; although this is technically demanding, the analysis is standard and conceptually straightforward. It will therefore be discussed elsewhere [10]. In particular, the real part of  $c_3$  is of importance for determining whether or not the flow is nonlinearly unstable: if  $\text{Re}c_3 < 0$ , then the nonlinear terms increase the damping of the amplitude and the unperturbed state is, within this approximation, also nonlinearly stable. On the other hand, if  $\text{Re}c_3 > 0$ , then the nonlinear term promotes the growth of the amplitude, and, in particular, amplitudes

$$|A| > A_c = \sqrt{\frac{\text{Im}\omega(k)}{\text{Re}c_3}} \quad (5)$$

grow without bound. Hence, in this approximation  $A_c$  constitutes the *critical amplitude beyond which the flow is nonlinearly unstable*. The results presented in Fig. 2(b) for  $A_c$  are obtained directly from our results for the coefficient  $c_3$ . In dimensionless units and with our normalization,  $A_c$  immediately yields the relative shear rate perturbation at the wall, necessary to make the flow unstable. With a numerical factor that we obtain from our analysis,  $A_c$  can be converted into a value for the critical relative shear stress ratio  $\tau_c$ , the perturbation in the shear stress beyond which the flow is unstable.

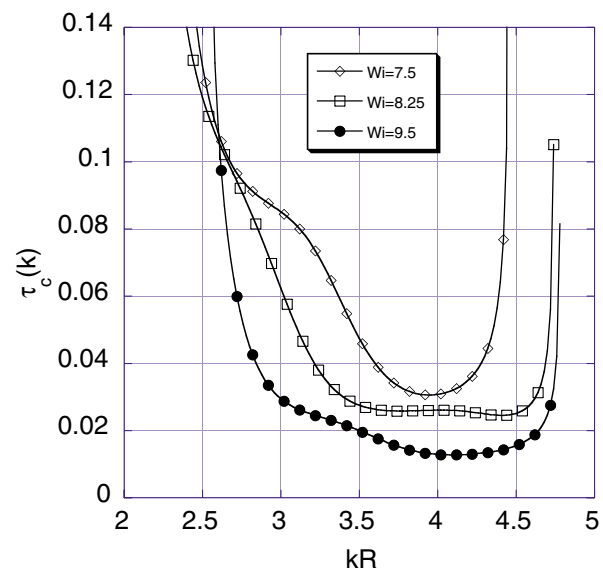


FIG. 3 (color online). Values of the critical shear stress amplitude  $\tau_c(k)$ , the ratio of the perturbation in the shear stress  $\tau_{rz}$  (normalized to the value  $\tau_{rz}^{\text{unp}}$  of the unperturbed state) at the wall above which the perturbation is nonlinearly unstable, as a function of the wave number  $k$  of the perturbation.

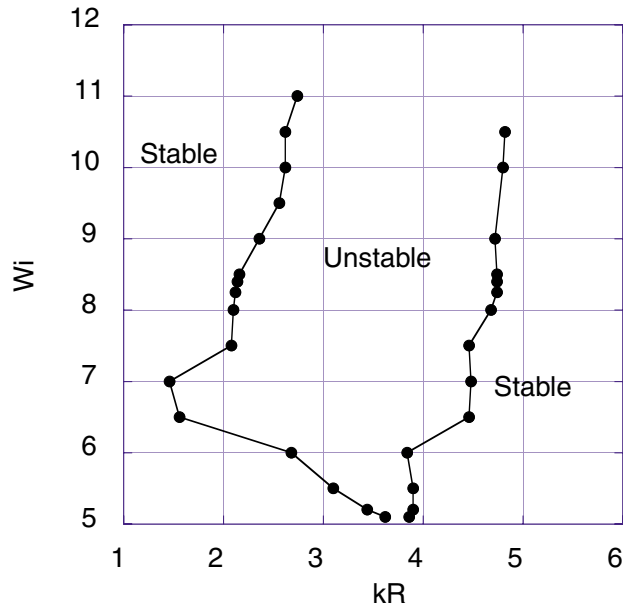


FIG. 4 (color online). Plot of the width of the  $k$  band where the corresponding modes render the basic Poiseuille flow profile unstable.

As we already discussed in connection with Fig. 2(b), for  $Wi \geq 5$ , we find that there is some range of wave numbers  $k$  for which  $Rec_3 > 0$ , and hence for which the Poiseuille profile is nonlinearly unstable. In Fig. 3 we show for three values of  $Wi$  the relative critical shear stress amplitude  $\tau_c(k)$  beyond which the flow is unstable, as a function of the wave number  $k$ . The further one gets above the value  $Wi_c$  where the instability sets in, the wider the band of  $k$  values is where we find an instability; the values plotted in Fig. 2(b) for  $\tau_c$  correspond to the minimum values of the curves in Fig. 3, but, as this figure shows for larger values of  $Wi$ , the bands are very flat so that the strength of the instability does not appear to depend very sensitively on  $k$  within the unstable band.

In Fig. 4 we plot the band in which modes are nonlinearly unstable beyond some threshold amplitude. It is important to realize that  $k$  in this figure is the wave number of the modulation of the Poiseuille flow *inside* the tube: Since the flow changes upon exiting the tube, this is not necessarily the same as the wave number of the induced roughness modulation outside the die, as in Fig. 1(c), but the two can be connected by equating the *frequency* of the modulations measured at a fixed position. Our numerical results show that the mode with  $kR \approx 3.75$ , which according to Fig. 4 emerges at  $Wi = Wi_c \approx 5$ , moves with a velocity of about  $v \approx 1.9v_{av}$ , where  $v_{av}$  is the average flow velocity. If the nonlinearities do not change this speed too much, this suggests a frequency  $f$  at onset of about  $3.75v/(2\pi R) \approx 1.13v_{av}/R$ . Further above threshold our amplitude expansion to cubic order neither yields the speed of the finite-amplitude modulated

stress pattern nor the selected wave number. However, it is reasonable to assume that in the saturated nonlinear regime, the pattern moves with speed  $v_{av}$  in the tube. From the band of unstable wave numbers shown in Fig. 4, we then conclude that the frequency of the extrudate modulations should then lie in the range  $0.3v_{av}/R \leq f \leq 0.72v_{av}/R$ .

The fact that the critical Weissenberg number  $Wi_c \approx 5$  which we find is in good agreement with the transition value noted empirically [4] is already a strong indication that the instability which we have identified lies at its origin. Further independent evidence comes from a series of new experiments which we have performed on a range of PVA (polyvinyl alcohol) Borax polymer solutions, whose rheological behavior is well described by the Oldroyd-B/UCM model. Our scenario implies that the first transition to melt fracture should be hysteretic, i.e., occur at a higher value of  $Wi$  upon increasing the flow rate than upon decreasing the flow rate; this is indeed observed in the experiments. Likewise, the wavelength of the roughness modulations is in good agreement with the theoretical analysis [1].

\*Present address: CWI, Postbus 94079, 1090 GB Amsterdam, The Netherlands.

†Present address: Department of Physics and Astronomy, University of Pennsylvania, Philadelphia, PA 19104.

- [1] V. Bertola, B. Meulenbroek, C. Wagner, C. Storm, W. van Saarloos, and D. Bonn (unpublished).
- [2] M. M. Denn, *Annu. Rev. Fluid Mech.* **22**, 13 (1990).
- [3] M. M. Denn, *Annu. Rev. Fluid Mech.* **33**, 265 (2001).
- [4] M. Pahl, W. Gleissle, and H.-M. Laun, *Praktische Rheologie der Kunststoffe und Elastomere* (VDI Verlag, Düsseldorf, 1991).
- [5] G.V. Vinogradov and V.N. Manin, *Kolloid Z.* **201**, 93 (1965); A. Groisman and V. Steinberg, *Nature (London)* **405**, 53 (2000); R. G. Larson, *Nature (London)* **405**, 27 (2000).
- [6] R. B. Bird, R. C. Armstrong, and O. Hassager, *Dynamics of Polymeric Liquids* (Wiley, New York, 1987).
- [7] T. C. Ho and M. M. Denn, *J. Non-Newtonian Fluid Mech.* **3**, 179 (1978).
- [8] R. G. Larson, E. S. G. Shaqfeh, and S. J. Muller, *J. Fluid Mech.* **218**, 573 (1990).
- [9] E. S. G. Shaqfeh, *Annu. Rev. Fluid Mech.* **28**, 129 (1996).
- [10] B. Meulenbroek, C. Storm, and W. van Saarloos (to be published).
- [11] P. Pakdel and G. H. MacKinley, *Phys. Rev. Lett.* **77**, 2459 (1996).
- [12] A. Groisman and V. Steinberg, *Phys. Fluids* **10**, 2451 (1998).
- [13] P. Huerre and M. Rossi, in *Hydrodynamics and Nonlinear Instabilities*, edited by C. Godrèche and P. Manneville (Cambridge University Press, Cambridge, 1998).